



ELSEVIER

Available online at [www.sciencedirect.com](http://www.sciencedirect.com)

SCIENCE @ DIRECT®

Physica A 323 (2003) 19–41

PHYSICA A

[www.elsevier.com/locate/physa](http://www.elsevier.com/locate/physa)

## Magnitude and sign scaling in power-law correlated time series

Yosef Ashkenazy<sup>a,\*</sup>, Shlomo Havlin<sup>b</sup>, Plamen Ch. Ivanov<sup>a,c</sup>,  
Chung-K. Peng<sup>c</sup>, Verena Schulte-Frohlinde<sup>a</sup>, H. Eugene Stanley<sup>a</sup>

<sup>a</sup>Department of Physics, Center for Polymer Studies, Boston University, Boston, MA 02215, USA

<sup>b</sup>Department of Physics, Gonda-Goldschmied Center, Bar-Ilan University, Ramat-Gan, Israel

<sup>c</sup>Beth Israel Deaconess Medical Center, Harvard Medical School, Boston, MA 02215, USA

Received 11 December 2002

---

### Abstract

A time series can be decomposed into two sub-series: a magnitude series and a sign series. Here we analyze separately the scaling properties of the magnitude series and the sign series using the increment time series of cardiac interbeat intervals as an example. We find that time series having identical distributions and long-range correlation properties can exhibit quite different temporal organizations of the magnitude and sign sub-series. From the cases we study, it follows that the long-range correlations in the magnitude series indicate *nonlinear* behavior. Specifically, our results suggest that the correlation exponent of the magnitude series is a monotonically increasing function of the multifractal spectrum width of the original series. On the other hand, the sign series mainly relates to *linear* properties of the original series. We also show that the magnitude and sign series of the heart interbeat interval series can be used for diagnosis purposes. © 2003 Published by Elsevier Science B.V.

*PACS:* 87.10.+e; 87.80.+s; 87.90.+y

*Keywords:* Scaling; Magnitude correlations; Multifractal spectrum; Volatility; Nonlinearity

---

### 1. Introduction

A broad class of physical and biological systems exhibits complex dynamics associated with the presence of many components interacting over a wide range of time or

---

\* Corresponding author.

*E-mail address:* [ashkenaz@wind.mit.edu](mailto:ashkenaz@wind.mit.edu) (Y. Ashkenazy).

space scales. These often-competing interactions may generate an output signal with fluctuations that appear noisy and erratic but in fact possess long-range correlations with scale-invariant structure [1–3]. Examples from diverse fields of interest that follow scaling laws include certain DNA sequences [4–8], heart-rate dynamics [9–16], neuron spiking [17], human gait [18], long-time weather records [19–21], cloud structures [22,23], and econometric time series [24,25].

In a recent study [26], it was shown that the fluctuations in the dynamical output may be characterized by two components—magnitude (absolute value) and sign (direction). These two quantities reflect the underlying interactions in a system, and the resulting force of these interactions at each moment determines the magnitude and direction of the fluctuations.

Here, we study the two-point correlation (scaling) properties of the magnitude and sign series<sup>1</sup> of series with long-range correlations. We find that different time series with the same long-range two-point correlations may have different correlations in their magnitude series. Using a recent test for nonlinearity [27] we see that the long-range two-point correlations of a time series quantify the linear properties of the underlying process (see Appendix A). Thus, different physical and biological systems may follow similar two-point scaling laws although the nonlinear properties of the underlying stochastic processes may be different. We show that correlations in the magnitude series are also related to the nonlinearity of a time series. We demonstrate that these correlations are related to the multifractal spectrum width (see Appendix A for the definition of multifractal spectrum).

The analysis of the long-range correlations of the magnitude and sign series is demonstrated on two types of time series: (i) the “real-life” time series (the cardiac interbeat-interval series), and (ii) the synthetic time series with well-known multifractal properties. The time series (i) of the increments of successive heartbeat intervals is anticorrelated over a broad range of time scales, i.e., the power spectrum follows a power law in which the amplitudes of the higher frequencies are dominant [5,11,28,29].<sup>2</sup> The synthetic time series (ii) allows us to investigate how the multifractal properties of a time series are reflected by the magnitude series correlations.

The paper is organized as follows. First we describe the magnitude and sign decomposition method (recently developed in Ref. [26]) and interpret the correlations in the magnitude and sign series (Section 2). Next we study the linear and nonlinear properties of the original series by analyzing the correlations in the magnitude and sign series. We generate surrogate data out of the original data by basically randomizing the Fourier phases—a procedure which is known to destroy nonlinearities. We compare the

---

<sup>1</sup> Some time series are uncorrelated although their magnitude series are correlated; the magnitude/sign decomposition is also applicable for this kind of series. Certain econometric time series [25], e.g., are uncorrelated at long-range although the volatility (local standard deviation) series is long-range correlated. Analysis of the correlation properties in the magnitude series is applicable for such series.

<sup>2</sup> By long-range anticorrelations we also mean that the root mean square fluctuations function  $F(n)$  is proportional to  $n^\alpha$  where  $n$  is the window scale and the scaling exponent  $\alpha$  is smaller than 0.5. In contrast, for uncorrelated (or finite correlated) series,  $\alpha=0.5$ , while for correlated series,  $\alpha > 0.5$ . In the present study we integrate the series before applying the DFA scaling analysis and thus  $\alpha = 1.5$  indicates uncorrelated behavior while  $\alpha > 1.5$  ( $\alpha < 1.5$ ) indicates correlated (anticorrelated) behavior.

correlation exponents of the magnitude and sign series of the original and the surrogate data (Section 3) and conclude that the correlations in magnitude series mainly reflect the nonlinearity of the original series while the sign series is mainly related to the linear properties. We then study the relation between the correlations in the original series and the correlations in the decomposed magnitude and sign series (Section 4). To study what type of nonlinearity is revealed by the magnitude series we generate two examples of multifractal (nonlinear) noise (Section 5) and find that the magnitude series two-point correlation scaling exponent is related to the multifractal spectrum width of the original series.<sup>3</sup> We then show that the magnitude and sign scaling exponents of the heart interbeat increment series may be used to separate healthy individual and those with congestive heart failure. Finally, we summarize and draw conclusions from our results (Section 7).

## 2. Magnitude and sign decomposition—method and interpretation

Any long-range correlated time series  $x_i$  can be decomposed into two different sub-series [26,30] formed by the magnitude and the sign of the *increments*

$$\Delta x_i \equiv x_{i+1} - x_i, \quad (1)$$

(see, e.g., Fig. 1). Here we perform detrended fluctuation analysis (DFA) [5,11] to find the correlations in the magnitude and sign sub-series.

The DFA procedure involves the following steps. The time series is integrated after subtracting the global average and then divided into windows of equal size  $n$ . In each window the data are fitted with a least-square polynomial curve [15] that represents the local trend in that window. In  $l$ th-order DFA, the polynomial has degree  $l$ . The integrated time series is detrended by subtracting the local polynomial trend in each window. The root mean square fluctuation  $F(n)$  of the integrated and detrended time series is calculated for different window sizes; when  $F(n) \sim n^\alpha$ , the two-point scaling exponent is  $\alpha$ . A long-range correlated series has exponent  $\alpha > 0.5$ , an uncorrelated series exponent  $\alpha = 0.5$ , and an anticorrelated series exponent  $\alpha < 0.5$ .

The correlation analysis of the magnitude and sign decomposition consists of the following steps:

- (i) From a given time series  $x_i$  we create the increment series  $\Delta x_i$ .<sup>4</sup>

---

<sup>3</sup> Here we study one type of nonlinearity, namely, long-range (scaling) nonlinearity. The long-range (scaling) linearity/nonlinearity is defined by the linear/nonlinear relation between the scaling exponents  $\tau(q)$  of different moments  $q$  (see Appendix A). Short-range nonlinear systems, like chaotic systems, are uncorrelated at long range and do not exhibit long-range nonlinear behavior; thus systems like chaotic systems require different techniques to reveal their finite-range nonlinear properties.

<sup>4</sup> For anticorrelated series, the original series  $x_i$  may be treated as the increment series. In the case that the increment series is correlated with DFA exponent  $\alpha > 0.5$  it is necessary to differentiate the series until it becomes anticorrelated with exponent  $\alpha < 0.5$ .

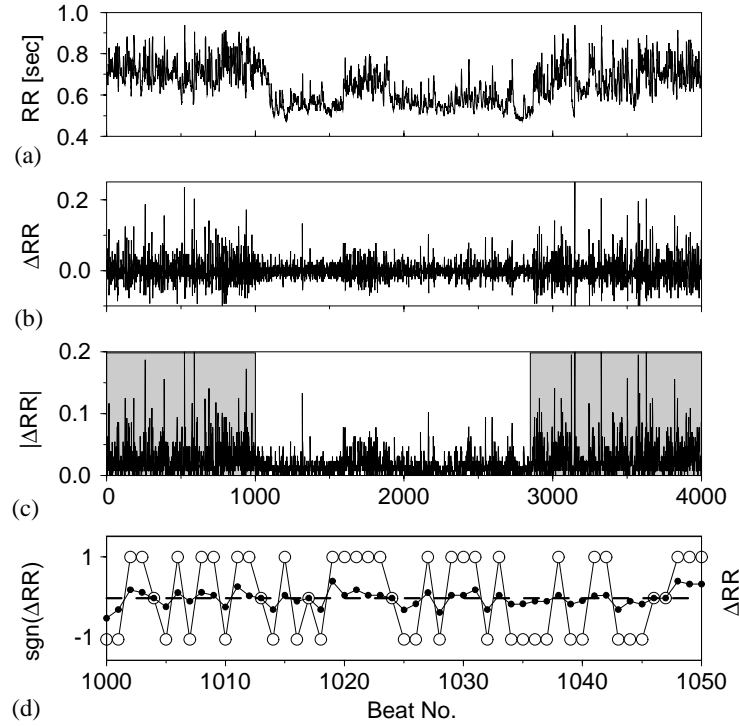


Fig. 1. (a) An example of 4000 heartbeat ( $RR$ ) intervals of a healthy subject during daytime. (b) The increment series of the  $RR$  series shown in (a). (c) The magnitude series of the  $RR$  series shown in (a). Patches of more “volatile” increments with large magnitude (shaded area) are followed by patches of less volatile increments with small magnitude, consistent with our quantitative conclusion that there is correlation in the magnitude time series. (d) The sign ( $\text{sgn}$ ) series (O), as well as the  $\Delta RR$  series (●) of a portion of the  $RR$  series (beat numbers 1000–1050) shown in (a). The positive sign (+1) represents a positive increment, while the negative sign (−1) represents a negative increment in the  $RR$  series of interbeat intervals. The tendency to alternation between +1 and −1 is consistent with our quantitative conclusion that there is (multiscale) anticorrelation in the sign time series.

- (ii) We decompose the increment series into a magnitude series  $|\Delta x_i|$  and a sign series  $\text{sgn}(\Delta x_i)$ ,<sup>5</sup>

$$\Delta x_i = \text{sgn}(\Delta x_i) |\Delta x_i|. \quad (2)$$

- (iii) To avoid artificial trends we subtract from the magnitude and sign series their respective means.  
 (iv) Because of limitations in the accuracy of the DFA method for estimating the scaling exponents of anticorrelated series (with scaling exponent  $\alpha < 0.5$ ), we first integrate the magnitude and sign series. The integrated series are thus correlated and their correlation exponents can be estimated accurately using the DFA method.<sup>6</sup>

<sup>5</sup> The function  $\text{sgn}(x)$  for  $x = 0$  might be defined to be +1, 0, or −1. Here we choose  $\text{sgn}(0) = 0$ .

<sup>6</sup> If, under rare circumstances, the integrated series is still anticorrelated, it is necessary to repeat steps (iii) and (iv) until the integrated magnitude/sign series become correlated.

- (v) We perform a scaling analysis using second-order DFA on the integrated magnitude and sign series.<sup>7</sup>
- (vi) To obtain the scaling exponents for the magnitude and sign series we calculate the slope of  $F(n)/n$  from a log–log plot. We use the normalized fluctuation function  $F(n)/n \sim n^{\alpha-1}$  to compensate for the additional integration from step (iv). This enables us to interpret the scaling results on the level of the increment series  $[\Delta x_i, |\Delta x_i|, \text{sgn}(\Delta x_i)]$  instead of on the level of the integrated series.

As a physiological example, we analyze the heart rate data (Fig. 1) for a group of 18 healthy individuals<sup>8</sup> for which it is known [11] that the heartbeat increment time series is anticorrelated (Figs. 3a and 4a). We find that the magnitude series exhibits *correlated* behavior (Figs. 3b and 4b). The sign series, however, exhibits *anticorrelated* behavior for window scales smaller than 100 beats (Figs. 3c and 4c); for scales larger than 100 beats the sign series gradually becomes uncorrelated.

Correlation in the magnitude series indicates that an increment with large (small) magnitude is more likely to be followed by an increment with large (small) magnitude. Anticorrelation in the sign series indicates that a positive increment is more likely to be followed by a negative increment and vice versa. Thus, our result for the temporal organization of heartbeat fluctuations suggests that, under healthy conditions, a large magnitude increment in the positive direction is more likely to be followed by a large magnitude increment in the negative direction. We find that this empirical “rule” holds over a broad range of time scales from several beats up to  $\sim 100$  beats (Fig. 3) [26,31].<sup>9</sup>

### 3. Linearity and nonlinearity as reflected by the magnitude and sign series

Scaling laws that are based on two-point correlations cannot reflect the nonlinearity of a series (see Appendix A) but, as we will show, the two-point correlations in the magnitude series do reflect the nonlinearity of the original series. For this purpose, we generate surrogate data out of a heartbeat interval increment time series using a technique that preserves the two-point correlations (as reflected by the power spectrum) and the histogram (but not the nonlinearities [32]). Comparison of the original time series with the surrogate time series shows that fluctuations with an identical scaling law can exhibit different correlations for the magnitude series.

---

<sup>7</sup> The first-order DFA eliminates constant trends from the original series (or, equivalently, linear trends from the integrated series) [5,11]; the second-order DFA removes linear trends, and the  $n$ th-order DFA eliminates polynomial trends of order  $n - 1$ .

<sup>8</sup> MIT-BIH Normal Sinus Rhythm Database and BIDMC Congestive Heart Failure Database available at <http://www.physionet.org/physiobank/database/#ecg>.

<sup>9</sup> Heartbeat increment series were investigated by A. Babloyantz and P. Maurer [31]. These studies differ from ours because we investigate, quantitatively, normal heartbeats by evaluating the scaling properties of the magnitude and sign series. In addition, our calculations are based on window scales larger than six and up to 1000 heartbeats.

A basic approach to creating surrogate data with the same scaling law as the original data is to perform a Fourier transform on the time series, preserving the amplitudes but randomizing the Fourier phases, and then to perform an inverse Fourier transform to create the surrogate series. This procedure should eliminate nonlinearities stored in the Fourier phases, preserving only the linear features of the original time series [33]. However, this does not preserve the probability distribution of the time series and may lead to an erroneous conclusion regarding the nonlinearity of the underlying process [27].

A technique which eliminates the nonlinearity of the original data but keeps the same power spectrum and histogram as the original was suggested in Ref. [32]. The procedure is iterative and consists of the following steps:

- (i) Store a sorted list of the original data  $\{x_i\}$  and the power spectrum  $\{S_k\}$  of  $\{x_i\}$ .
- (ii) Begin ( $l = 0$ ) with a random shuffle  $\{x_i^{(l=0)}\}$  of the data.
- (iii) Replace the power spectrum  $\{S_k^{(l)}\}$  of  $\{x_i^{(l)}\}$  by  $\{S_k\}$  (keeping the Fourier phases of  $\{S_k^{(l)}\}$ ) and then transform back.
- (iv) Sort the series obtained from (iii).
- (v) Replace the sorted series from (iv) by the sorted  $\{x_i\}$  and then return to the pre-sorting order [i.e., the order of the series obtained from (iii)]; the resulting series is  $\{x_i^{(l+1)}\}$ .

Repeat steps (iii)–(v) until convergence (i.e., until series from consecutive iterations will be almost the same).<sup>10</sup>

We iterate steps (iii)–(v) 100 times to create surrogate data of heartbeat increment series (Fig. 2); we use 100 iterations to make sure that convergence is achieved. Nonetheless, in some cases, few iterations may be sufficient for convergence. We apply the surrogate test to the increment series and not to the original series in part because the increment series is stationary (i.e., the variance of the series remains finite when increasing the series length to infinity) and is thus more appropriate for the use of the surrogate data test. The new surrogate series (Fig. 2a) has almost the same fluctuation function  $F(n)$  as the original heartbeat increment series, with a scaling exponent indicating long-range anticorrelations in the interbeat increment series (Fig. 3a). Our analysis of the sign time series derived from the surrogate series (Fig. 2c) shows scaling behavior almost identical to the scaling of the sign series derived from the original data (Fig. 3c). On the other hand, the magnitude time series derived from the surrogate (linearized) signal (Fig. 2b) exhibits *uncorrelated* behavior—a significant change from the strongly *correlated* behavior observed for the original magnitude series (Fig. 3b). Thus, the increments in the surrogate series do not follow the empirical “rule” observed for the original heartbeat series, although these increments follow a scaling law

---

<sup>10</sup> Another test for nonlinearity [34] consists of the following steps: (i) create a Gaussian white noise, (ii) reorder it as the original series, (iii) phase-randomize the series, and (iv) reorder the original series according to the series from (iii). The surrogate series from (iv) has the same distribution and similar power spectrum as the original series; however, this procedure does not accurately preserve the low frequencies in the power spectrum [32] and thus is not applicable for series with long-range correlations.

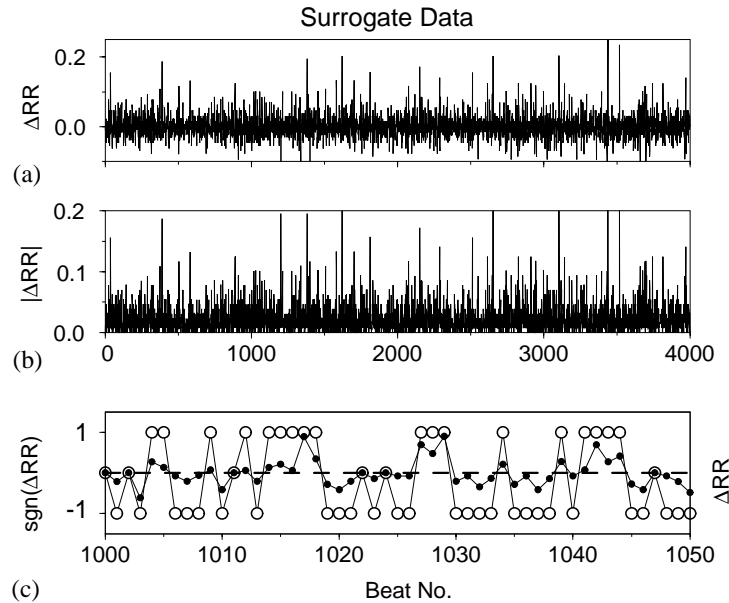


Fig. 2. (a) The surrogate data of the  $\Delta RR$  series shown in Fig. 1b. The surrogate increment series has almost the same two-point correlations and the same probability distribution but random Fourier phases. The surrogate series is more homogeneous than the original  $\Delta RR$  series. (b) The magnitude series decomposed from the series shown in (a). The magnitude series is homogeneous and does not show the patches of small and big magnitude values shown in Fig. 1c. This suggests that the “clustering” of the magnitude series is a measure of nonlinearity. (c) A portion of the sign series of the series shown in (a). The sign series shows similar alternations as in the original sign series (Fig. 1d).

identical to the original heartbeat increment series. Our results indicate that the magnitude series carries information about the nonlinear properties of the original heartbeat series, while the sign series relates mainly to linear properties.

To further validate these results, we apply the surrogate data test for nonlinearity to the heartbeat increment series (daily records) of the 18 healthy subjects discussed above (see footnote 8). For each of the 18 individuals we find that the DFA scaling exponent of the surrogate data is very close to (although slightly higher than) the exponent of the original data (Fig. 4a). The small discrepancies between the surrogate data exponents and the original data exponents might be a result of the finite length and finite resolution of the interbeat interval series. The magnitude exponent of the surrogate data indicates uncorrelated behavior (scaling exponent of  $\alpha - 1 \approx 0.5$ ) for each of the subjects (Fig. 4b) in contrast to the correlations found in the magnitude series of the original data. This drastic change from correlated to uncorrelated behavior for all subjects confirms our result that the magnitude series carries information about nonlinear properties of the original data. In Section 5, we show that this type of nonlinearity is related to multifractality. The sign series exponent of the surrogate data remains almost unchanged after the surrogate data test (Fig. 4c). Thus, the sign series seems mainly to reflect the linear properties of the original series.

The difference between the exponents before and after the surrogate data test for nonlinearity may be quantified as follows. If  $\alpha$  is the exponent derived from the original

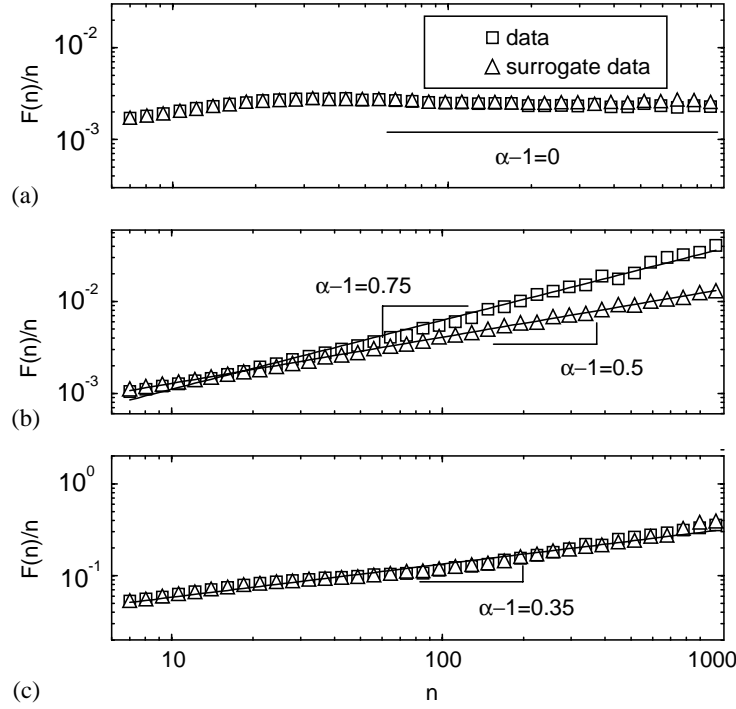


Fig. 3. (a) Root mean square fluctuation,  $F(n)$ , for  $\approx 6$  h record ( $\approx 32\,000$  data points) for the interbeat interval  $RR$  series ( $\square$ ) of the healthy subject shown in Fig. 1. Here,  $n$  indicates the time scale (in beat numbers) over which each measure is calculated. The scaling is obtained using second-order detrended fluctuation analysis, and indicates (since  $\alpha - 1 = 0$ ) long-range anticorrelations in the heartbeat interval increment series  $\Delta RR$  [11,15]. By construction, the scaling properties of the interval increment series remain almost unchanged after the surrogate data test ( $\triangle$ ). (b) The root mean square fluctuation,  $F(n)$ , of the integrated magnitude series ( $\square$ ) indicates long-range correlations in the magnitude series  $|\Delta RR|$  (group average exponent of  $\alpha - 1 = 0.74 \pm 0.08$  where  $F(n)/n \propto n^{\alpha-1}$ ). After a surrogate data test applied to the interbeat interval increment series we find uncorrelated behavior with exponent 0.5 ( $\triangle$ ). This change in the scaling suggests that the magnitude series carries information about the nonlinear properties of the original series since the nonlinear properties are removed by the surrogate test procedure. (c) The root mean square fluctuation of the integrated sign series ( $\square$ ) indicates short-range ( $7 \leq n \leq 64$ ) anticorrelated behavior in  $\text{sgn}(\Delta RR)$  series (group average exponent of  $\alpha - 1 = 0.32 \pm 0.06$  where  $F(n)/n \propto n^{\alpha-1}$ ). The scaling properties of the sign series remain unchanged after the surrogate data test ( $\triangle$ ), which suggests that the sign series relates to linear properties of the original time series. We note the apparent crossovers at  $n \approx 20$  beats and  $n \approx 100$  beats. At larger scales ( $n > 64$ ) the sign series loses its specificity and converges gradually to  $\alpha - 1 \approx 0.5$ . Thus, the sign series correlation properties may reveal significant information only for scales  $n < 100$ . We note, however, that heartbeat increments derived from the original time series are anticorrelated up to scales of thousands of heartbeats.

data and  $\bar{\alpha}_s$ ,  $\Delta\alpha_s$  are the average and the standard deviation of the exponents derived from the surrogate data, then the separation is given by [34]

$$\sigma = |\alpha - \bar{\alpha}_s| / \Delta\alpha_s. \quad (3)$$

$\sigma$  measures how many standard deviations the original exponent is separated from the surrogate data exponent. The larger the  $\sigma$  the larger the separation between the exponents derived from the surrogate data and the exponent derived from the original data. Thus, larger  $\sigma$  values indicate stronger nonlinearity. In Fig. 4d we show the  $\sigma$

values for the magnitude and sign exponents. The  $\sigma$  values of the magnitude exponents are large and thus indicate a significant difference between the magnitude exponents of the original and the surrogate data. On the other hand the  $\sigma$  values of the sign exponents are small, indicating similarity between the sign exponents of the original and surrogate data. Thus, we conclude that the magnitude series indicates nonlinearity of the original data. The sign series, on the other hand, relates mainly to the linear properties.

#### 4. The relation between the original, magnitude, and sign series scaling exponents

Recently [26], we investigated the relation between the scaling exponent of the original series and the scaling exponents of the integrated magnitude series and the integrated sign series. We generated long-range correlated linear noise with different scaling exponents ranging from  $\alpha = 0.5$  to 1.5. Then we decomposed the increment series into a magnitude series and a sign series. Finally, we calculated the scaling exponents of the integrated magnitude and sign series. At small time scales ( $n < 16$ ), we found an empirical approximate relation for the scaling exponents,

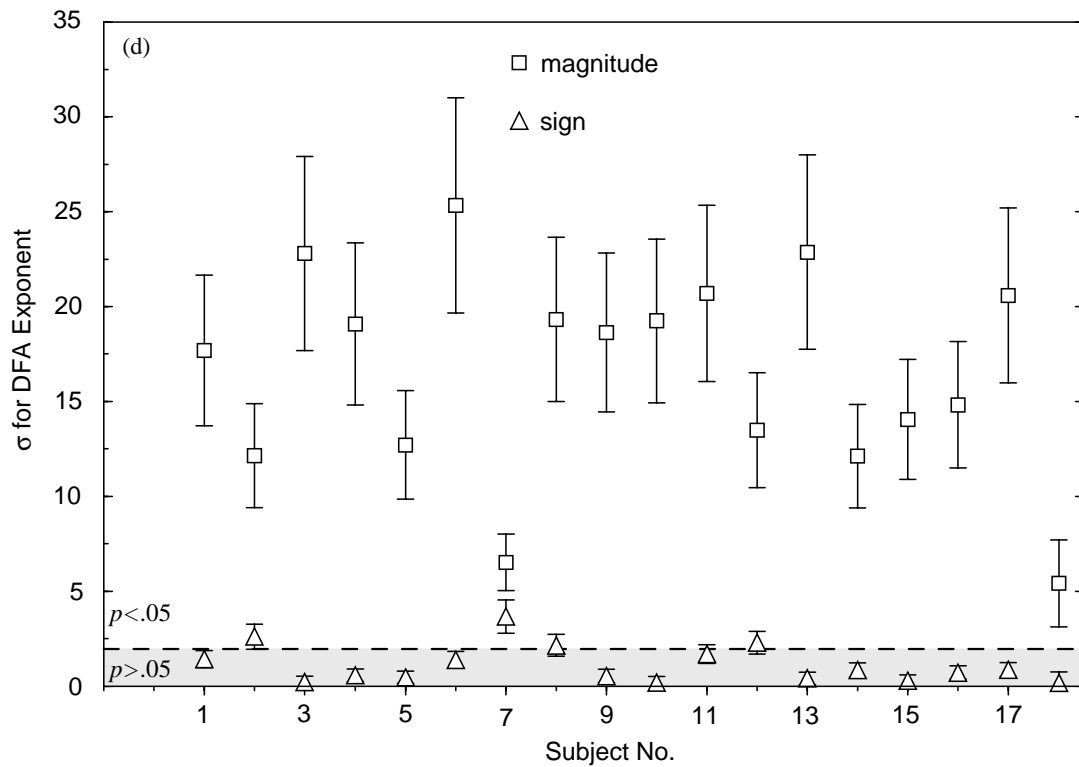
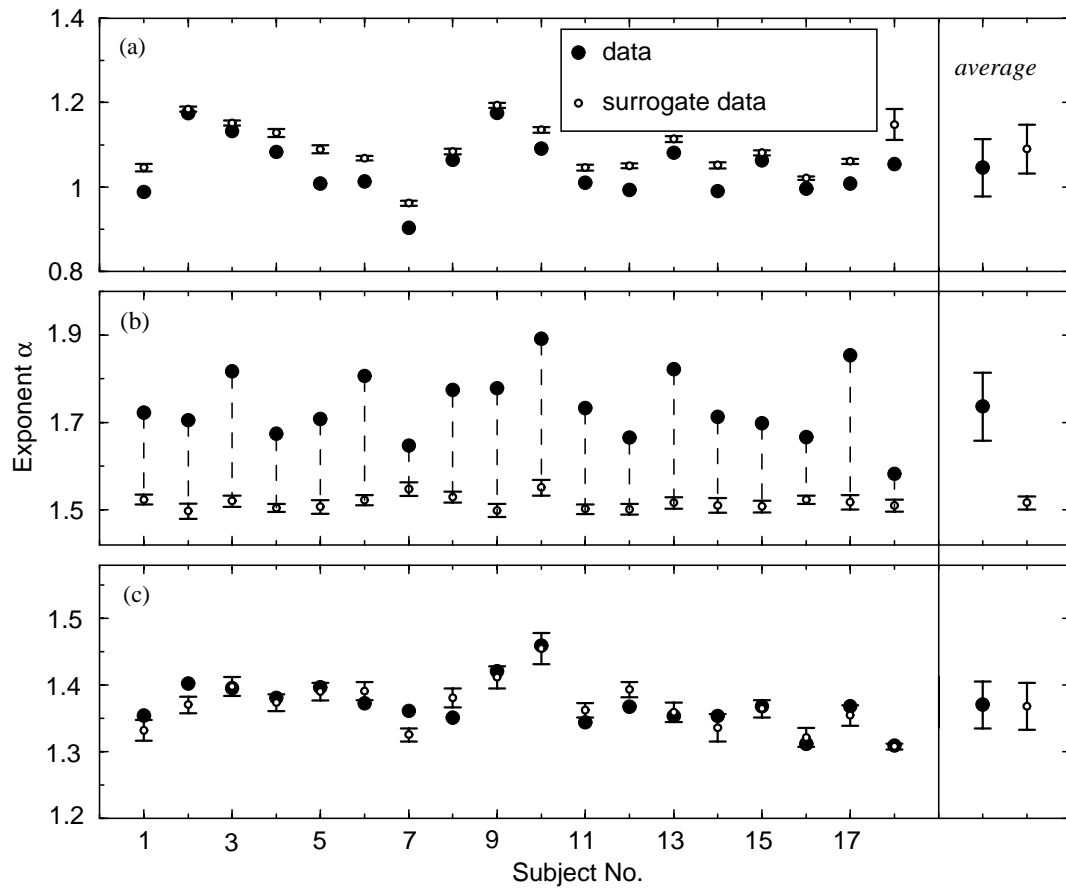
$$\alpha_{\text{sign}} \approx \frac{1}{2}(\alpha_{\text{original}} + \alpha_{\text{magnitude}}). \quad (4)$$

At larger window scales ( $n > 64$ ), we find that for linear noise with a scaling exponent  $\alpha < 1.5$ , the magnitude and sign series of the increments are uncorrelated. In the following we suggest an explanation for these findings. We also show that, for  $\alpha > 1.5$  in the original series, the integrated magnitude series and the integrated sign series have approximately the same two-point scaling exponent.

We observe uncorrelated behavior for the magnitude series since we use *linear* noise (see Section 3 where we find that uncorrelated behavior of the magnitude series reflects linearity of the original series). In the next section, we show that the magnitude series is correlated for multifractal nonlinear noise. The sign series exhibits anticorrelated behavior for small scales and uncorrelated behavior for larger scales, regardless of the nonlinear properties of the original time series.

At small scales, the sign series coarse grains the increment series and thus preserves some of its correlation properties. For instance, if the increment series is anticorrelated, i.e., a large increment value is followed by a small increment value, the sign series will also alternate and be anticorrelated. On the other hand, if the increment series is uncorrelated, the sign series will also perform random behavior and be uncorrelated.

The power spectrum of long-range anticorrelated series *increases* in power-law manner. This implies that the amplitudes of low frequencies are much smaller than the amplitudes of higher frequencies. The crude coarse graining of the increment series by the sign series mainly approximates the high frequency band (small window scales) since the majority of the power spectrum lays in this frequency band. However, the sign series cannot maintain the very small amplitudes of the low frequencies (long-range anticorrelations) due to the small fraction of the power spectrum at this frequency band. This may lead to uncorrelated behavior of the sign series for larger window scales.



For correlated noise with scaling exponents larger than 1.5 (i.e., the increment series is also correlated with an exponent larger than 0.5) the scaling exponents of the original series, the integrated magnitude series, and the integrated sign series all tend to converge to the same value (Fig. 5a, and b). An intuitive explanation for this finding follows.

Correlated series are persistent: large values are followed by large values. This implies that the correlated increment series crosses the  $x$ -axis only a few times. Thus, the magnitude series will preserve the profile of the increment series up to the few points where crossings with the  $x$ -axis occur. As a result, the magnitude series will preserve the correlations of the increment series; the crossings with the  $x$ -axis will cause a small deviation from the original correlations.

Since the increment series is also long-range correlated, its power spectrum *decays* in power-law manner; the amplitudes of low frequencies are much larger than the amplitudes of high frequencies. The sign series captures the majority of the power spectrum which lays in the low frequency regime (large window scales) and thus tends to follow the long-range correlations of the original increment series.

## 5. Relation between correlations in magnitude series and the multifractal spectrum width

In Section 3 we proposed that the magnitude series scaling exponent is related to nonlinear properties of the original series, while the sign series exponent is related to

---

Fig. 4. A summary of the surrogate data test for nonlinearity applied for the interbeat interval ( $RR$ ) series. The surrogate data ( $\circ$ ) has the same linear properties as the original data ( $\bullet$ ); the nonlinear properties of the original series are destroyed by the surrogate data test. For each of the 18 healthy records (16384 data points each) we produce 10 realizations of surrogate data and calculate the scaling exponents of the original  $RR$  series, the magnitude series, and the sign series (the scaling exponents are calculated in the range  $6 < n < 1024$ ). (a) The scaling exponent of the original  $RR$  series and surrogate  $RR$  series. The scaling exponent is preserved after the surrogate data test. The group averages  $\pm$  standard deviation, on the right, show similar values both for the original data and the surrogate data. (b) The scaling exponents of the integrated magnitude series decomposed from the original  $RR$  and surrogate  $RR$  series. The magnitude series of the original series is correlated ( $\alpha - 1 \sim 0.75$ ) whereas the magnitude series of the surrogate data is uncorrelated ( $\alpha - 1 \sim 0.5$ ). This significant change indicates that the magnitude series carries information regarding the nonlinear properties of the underlying mechanism. (c) Same as (b) for the sign series. Here the exponent derived from the surrogate series coincides with the original sign scaling exponent. This indicates that the sign series mainly reflect the linear properties of the underlying (heartbeat) dynamics. Note that although the sign series fluctuation function exhibits a crossover and converges to uncorrelated behavior at large scales ( $n > 64$ , see Fig. 3c), we calculate the scaling exponent for the entire regime ( $6 \leq n \leq 1024$ ) to emphasize that the surrogate data test does not affect the sign scaling in *all* scaling regimes. (d) A measure for the separation between the original and surrogate data magnitude and sign exponents—large  $\sigma$  value indicates big difference between the original data and the surrogate data exponents. The gray area at the bottom indicates  $\sigma$  values with  $p$ -value more than 0.05 (statistical similarity) while  $\sigma$  values above the gray area indicate significant difference between the original series exponents and the surrogate data exponents (see Ref. [34] for details). Here we show that the original magnitude series exponent is significantly different from the surrogate magnitude series exponent while the sign series exponent of the original data and the surrogate data are statistically similar.

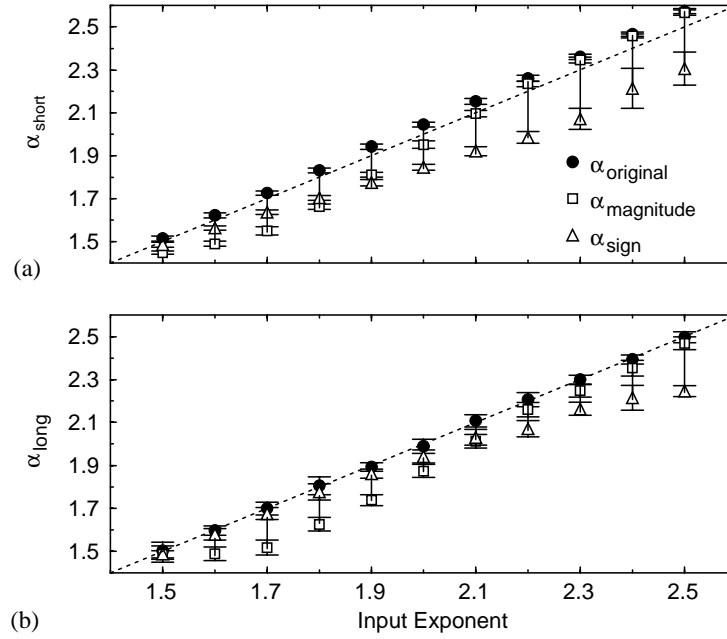


Fig. 5. (a) The relation between the scaling exponents of correlated noise, the integrated magnitude series, and the integrated sign series for the short-range regime ( $n < 16$ ). We generate 10 series of length 32 768 with specific correlations (input exponent) and then calculate the scaling exponents of the original series ( $\bullet$ ), of the integrated magnitude series ( $\square$ ), and of the integrated sign series ( $\triangle$ ); the average  $\pm 1$  standard deviation are shown. All three exponents tend to converge to the same value. (b) Same as (a) for the long-range regime ( $64 < n < 1024$ ). Also in this regime the scaling exponents of the original, magnitude, and sign series tend to converge to the same value.

linear properties. Here we study what type of nonlinearity is revealed by the magnitude series correlations.

Linear series with long-range correlations are characterized by linearly dependent  $q$ -order correlation exponents  $\tau(q)$ , i.e., the exponents  $\tau(q)$  of different moments  $q$  are *linearly* dependent,

$$\tau(q) = Hq + \tau(0), \quad (5)$$

with a single Hurst exponent,<sup>11</sup>

$$H \equiv d\tau/dq = \text{const}. \quad (6)$$

In this case the series is called *monofractal*. Long-range correlated nonlinear signals have a multiple Hurst exponent

$$h(q) \equiv d\tau/dq \neq \text{const}, \quad (7)$$

where  $\tau(q)$  depends *nonlinearly* on  $q$ . In this case the series is called *multifractal* (MF). The MF spectrum is defined by

$$D(h) = h(q)q - \tau(q), \quad (8)$$

<sup>11</sup> The DFA exponent  $\alpha = H + 1$  and the second moment  $\tau(2) = 2H + \tau(0) = 2\alpha - 2 + \tau(0)$ . For continuous series  $\tau(0) = -1$  and thus  $\tau(2) = 2\alpha - 3$ .

where, for a monofractal series, it collapses to a single point,

$$D(H) = -\tau(0) . \quad (9)$$

Here we show the nonlinear measure of the magnitude series scaling exponent to be related to the MF spectrum  $D(h)$ .

Indeed, a previous study [14] showed that the healthy heartbeat interval series is MF and indicated that after Fourier-phase randomization the interbeat interval series becomes monofractal. Moreover, this study also indicated a loss of multifractality with disease—heart failure patients have a narrower MF spectrum than healthy individuals. Comparison of the magnitude series scaling exponent of healthy and heart failure individuals shows significantly higher exponents for healthy subjects [26]. This result is additional numerical (although not mathematical) evidence showing that the magnitude series scaling exponent may be related to the MF spectrum. The change in the magnitude exponent for heart failure subjects is also consistent with a previously reported loss of nonlinearity with disease [14,35,36].

In order to test the connection between the magnitude scaling exponent and the MF spectrum, we generate artificial noise with built-in MF properties. Then we check how the magnitude scaling exponent is related to the MF spectrum width.

We use the algorithm proposed in Ref. [37] to generate the artificial MF noise. This algorithm is based on random cascades on wavelet dyadic trees. Briefly, the random MF series is built by specifying its discrete wavelet coefficients  $c_{j,k}$ . The coefficient  $c_{j,k}$  is defined recursively as

$$\begin{aligned} c_{0,0} &= 1 , \\ c_{j,2k} &= Wc_{j-1,k} , \\ c_{j,2k+1} &= Wc_{j-1,k} \end{aligned} \quad (10)$$

for all  $j$  ( $j \geq 1$ ) and  $k$  ( $0 \leq k < 2^{j-1}$ ), where  $W$  is a random variable. Once the wavelet coefficients  $c_{j,k}$  are constructed, we apply an inverse wavelet transform to generate MF random series. The MF properties of the series can be determined according to the distribution of the random variable  $W$ .

We consider two different types of probability distributions for the random variable  $W$ : the log-normal distribution and the log-Poisson distribution. For these two examples the MF properties are known analytically [37]. The MF spectrum  $D(h)$  is symmetric for the log-normal distribution and asymmetric for the log-Poisson distribution. We use the 10-tap Daubechies discrete wavelet transform [38,39].

### 5.1. Log-normal $W$ distribution

We consider the case of a log-normal random variable  $W$  where  $\ln|W|$  is normally distributed and  $\mu$ ,  $v^2$  are the mean and the variance of  $\ln|W|$ . For simplicity we choose  $\mu = -\frac{1}{4} \ln 2$ . In this case, the scaling exponent of different moments  $\tau(q)$  is

given by

$$\tau(q) = -\frac{v^2}{2 \ln 2} q^2 + \frac{q}{4} - 1 \quad (11)$$

and the MF spectrum  $D(h)$  is

$$D(h) = -\frac{(h - 1/4)^2 \ln 2}{2v^2} + 1. \quad (12)$$

The MF spectrum width can be found by solving  $D(h) = 0$  and is

$$h_{\max} - h_{\min} = \left( \frac{\sqrt{2}v}{\sqrt{\ln 2}} + \frac{1}{4} \right) - \left( -\frac{\sqrt{2}v}{\sqrt{\ln 2}} + \frac{1}{4} \right) = \frac{2\sqrt{2}v}{\sqrt{\ln 2}}. \quad (13)$$

Thus for  $v = 0$  the series will be monofractal and, for larger  $v$  values, will have a broader MF spectrum (Eq. (13)). It is also clear that for  $v \rightarrow 0$ ,  $D(H = 1/4) = 1$  (Eqs. (12), (13)), and for larger values of  $v$ , the MF spectrum is symmetric around  $D(1/4) = 1$  (Fig. 6a, b).

We generate series with different  $v$  values ranging from 0 to 0.1 (20 realizations for each  $v$ ) and calculate the original, magnitude, and sign scaling exponents (Fig. 6c). We find that indeed the original series exponent has a fixed value  $\approx 1.25$ ; this exponent is consistent with the Hurst exponent  $H = 0.25$  since the DFA exponent  $\alpha = H + 1$ . The sign series also has a fixed value  $\approx 1.45$  (see Ref. [26]). The magnitude series scaling exponent increases monotonically with  $v$  from uncorrelated magnitude series with scaling exponent  $\alpha - 1 \approx 0.5$  to strongly correlated magnitude series with exponent  $\alpha - 1 \approx 1$ . The magnitude exponent converges to  $\alpha - 1 = 1$ .

Since there is a linear relation between  $v$  and the MF spectrum width (Eq. (13)) and since the magnitude exponent increases monotonically with  $v$ , we suggest that the magnitude exponent is related to the MF spectrum width.

## 5.2. Log-Poisson $W$ distribution

In the previous section, we study an example with a symmetric MF spectrum  $D(h)$ . Here we show that changes in the magnitude scaling exponent are *not* a result of changes in the positive moments only (and especially the fourth moment) but rather reflect changes of the entire MF spectrum. For this purpose we study an example with an asymmetric MF spectrum where the exponents for negative moments,  $h(q < 0)$ , are changed drastically when the MF spectrum width is changed while  $h(q > 0)$  is less significantly changed. We tune the parameters in such a way that the fourth moment  $\tau(4)$  is fixed and the second moment  $\tau(2)$  is hardly changed.

We consider the case of a log-Poisson random variable  $W$ , where  $\lambda$  is the mean and also the variance of Poisson variable  $P$ , and  $\ln|W|$  has the same distribution function as  $P \ln \delta + \gamma$ ;  $\delta$  is an appropriately chosen positive parameter [37]. We choose  $\lambda = \ln 2$  and  $\gamma = -\delta^4 \ln 2/4$ . Under this choice of parameters,

$$\tau(q) = -\delta^q + q\delta^4/4 \quad (14)$$

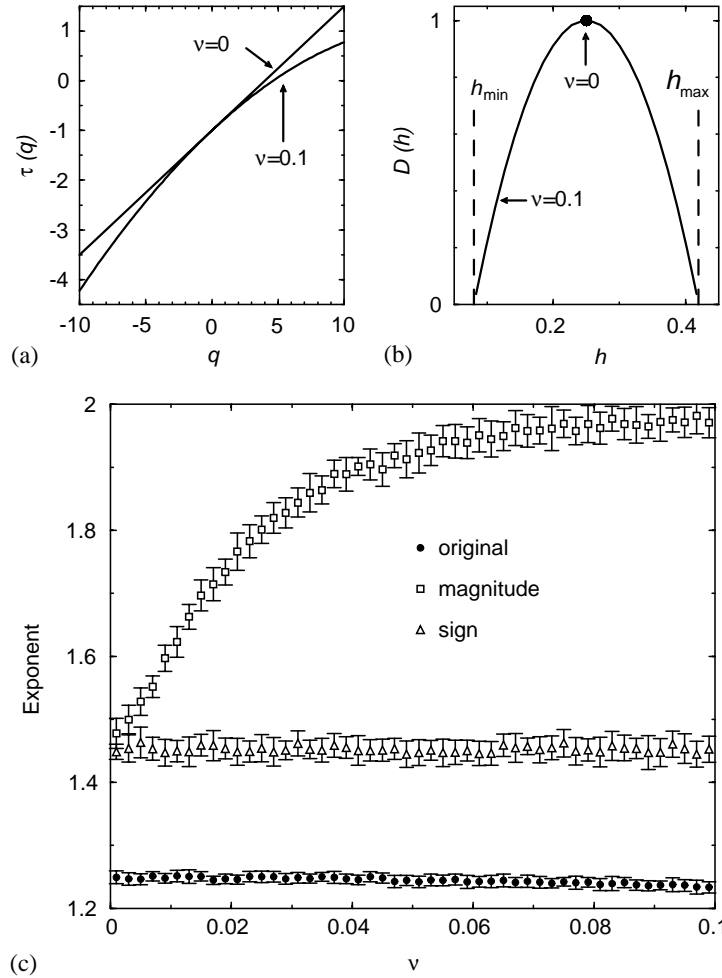


Fig. 6. A test on MF random series with log-normal distribution of wavelet coefficients. The artificial time series have symmetric MF spectrum; the width of the MF spectrum is proportional to  $v$ . (a) The theoretical scaling exponent  $\tau(q)$  for  $v=0$  and  $v=0.1$ . The linear  $\tau(q)$  ( $v=0$ ) indicates monofractality while the curved  $\tau(q)$  indicates multifractality. (b) The MF spectrum,  $D(h)$ , for the  $\tau(q)$  shown in (a). For  $v=0$  (●) the  $D(h)$  MF spectrum is a single point indicating monofractality; the global Hurst exponent is  $H=0.25$  (DFA exponent  $\alpha=1.25$ ). For  $v=0.1$  (curved solid line) the  $D(h)$  spectrum is wide indicating multifractality. The MF spectrum is symmetric and centered around  $h=0.25$ . The vertical dashed lines indicate the minimum ( $h_{\min}$ ) and maximum ( $h_{\max}$ ) local Hurst exponents. (c) The original, magnitude, and sign scaling exponents as a function of  $v$ . For each  $v$  value we generate 20 realizations each of 65 536 points. Then we calculate the different scaling exponents in the range  $64 \leq n \leq 4096$ ; the average exponent  $\pm 1$  standard deviation is shown. The original and sign scaling exponent remains almost constant while the magnitude scaling exponent gradually increases from 1.5 to 2. Since  $v$  is proportional to the MF spectrum width,  $h_{\max} - h_{\min}$ , we suggest that the magnitude scaling exponent is also related to the width of the MF spectrum.

and

$$D(h) = \frac{1}{\ln \delta} (h - \delta^4/4) \left[ \ln \left( \frac{h - \delta^4/4}{-\ln \delta} \right) - 1 \right]. \quad (15)$$

Thus, the fourth moment  $\tau(4)$  is independent of  $\delta$

$$\tau(4) = 0 \quad (16)$$

and the width of the MF spectrum depends on  $\delta$

$$h_{\max} - h_{\min} = (\delta^4/4 - e \ln \delta) - (\delta^4/4) = -e \ln \delta . \quad (17)$$

For  $\delta = 1$  the MF spectrum collapses and becomes a single point (monofractal) with Hurst exponent  $H=1/4$  and  $D(1/4)=1$ . For decreasing or increasing  $\delta$  the MF spectrum becomes wider. Here we change the MF spectrum width by decreasing  $\delta$ ; the major change in the MF spectrum occurs for negative moments  $q < 0$  (Fig. 7a and b).

In Fig. 7c we show the scaling exponents of the original, magnitude, and sign series for different values of  $\delta$ . We find that the original and sign series exponents hardly change with  $\delta$ , while the magnitude exponent increases monotonically. This increase suggests that the magnitude scaling exponent is related to the MF spectrum width (see also Fig. 6).

We summarize the results of the log-normal and the log-Poisson examples in Fig. 7d—the magnitude scaling exponent is plotted versus the width of the MF spectrum [Eqs. (13), (17)]. Surprisingly, these two examples collapse to the same curve. This collapse suggests a possible one-to-one relation<sup>12</sup> between the magnitude scaling exponent and the MF spectrum width.<sup>13</sup>

The relation between the magnitude scaling exponent and the MF spectrum width is consistent with a recent study of Bacry et al. [40]. It was shown there that it is possible to generate an MF series  $x_i$  with Gaussian random variables  $\varepsilon_l, \omega_l$ ,

$$x_i = \sum_{l=1}^i \Delta x_l = \sum_{l=1}^i \varepsilon_l e^{\omega_l} . \quad (18)$$

For correlated  $\omega_l$  the series  $x_i$  is MF, while for uncorrelated  $\omega_l$  it is monofractal. Stronger correlations in  $\omega_l$  yields broader MF spectrum. The magnitude series  $|\Delta x_l|$  is equivalent to the positive numbers  $e^{\omega_l}$  while the sign series may be represented by the real numbers  $\varepsilon_l$ . Thus, correlations in  $|\Delta x_l|$  may be related to correlations in  $e^{\omega_l}$  and both may be related to the MF spectrum width. We note that this comparison is qualitative since the sign series is a binary series (+1 or -1) while the  $\varepsilon_l$  is a continuously valued Gaussian random variable.

The results described in this section may be important from a practical point of view since the calculation of the MF spectrum from a time series involves advanced

<sup>12</sup> We define a one-to-one relation as follows: let  $y = f(x)$ , then if  $x$  is a single-valued function of  $y$  and  $y$  is a single-valued function of  $x$  then  $x$  and  $y$  are one-to-one related.

<sup>13</sup> We also performed the same procedure (as in Figs. 6, 7) for a deterministic multifractal object, namely the generalized devil's staircase [41]. Also here we find that magnitude exponent increases monotonically with the multifractal spectrum width. However, for very small multifractal width the magnitude exponent was  $\sim 1$  and then increased sharply to the behavior shown in Fig. 7d; this behavior might be related to the deterministic nature of this multifractal object.

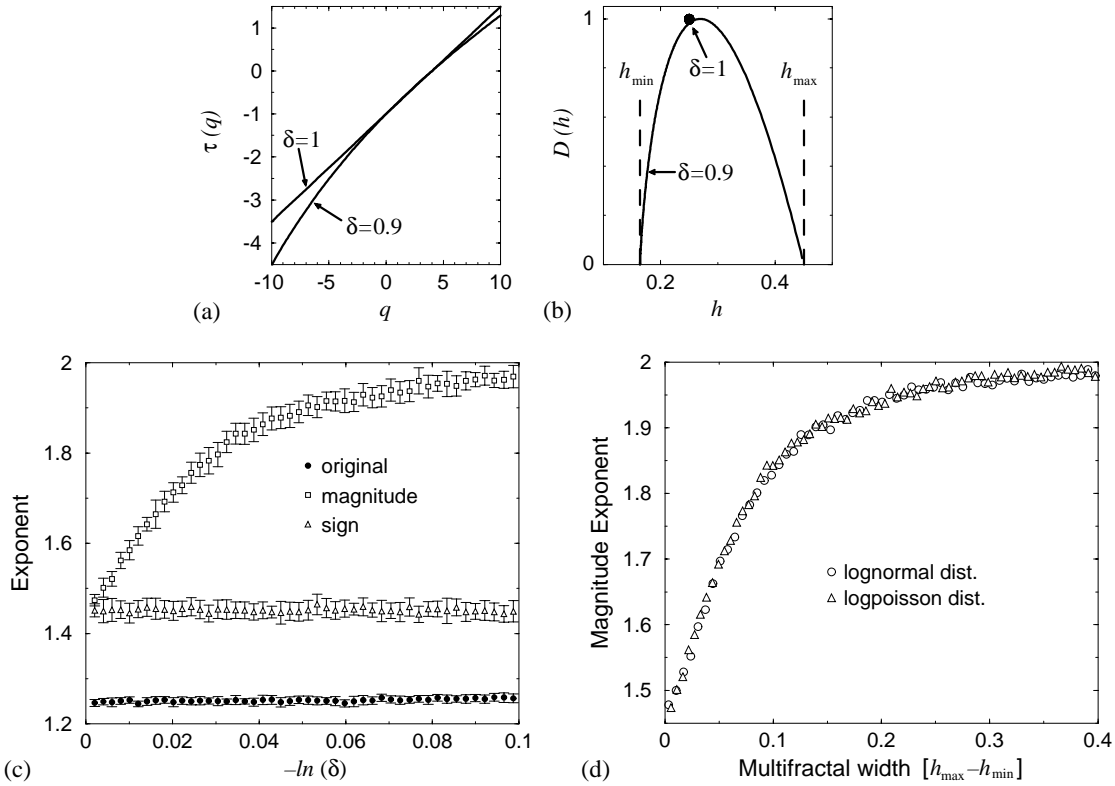


Fig. 7. Same as Fig. 6 for log-Poisson distribution of the discrete wavelet coefficients. We generate series with *asymmetric* MF spectrum where the second moment  $\tau(2)$  and the fourth moment  $\tau(4)$  are almost fixed. (a) The  $\tau(q)$  spectrum for  $\delta = 1$  (linear curve that indicates monofractality) and for  $\delta = 0.9$  (curved line that indicates multifractality). Note that for positive  $q$ 's  $\tau(q)$  is just slightly changed;  $\tau(q)$  is changed more significantly for negative  $q$ 's. (b) The MF spectrum  $D(h)$  for the examples shown in (a). The  $D(h)$  spectrum for  $\delta = 1$  is monofractal ( $\bullet$ ); the global Hurst exponent is  $H = 0.25$  (DFA exponent  $\alpha = 1.25$ ). For  $\delta = 0.9$  (solid curved line)  $D(h)$  MF spectrum is broad and asymmetric.  $D(h)$  is more stretched to the right indicating larger changes in the negative moments. The vertical dashed lines indicate the minimum ( $h_{\min}$ ) and maximum ( $h_{\max}$ ) local Hurst exponents. (c) Same as Fig. 6c. Here the MF spectrum width is proportional to  $-\ln \delta$ . The original and sign scaling exponents remain almost fixed as a function of  $\delta$  while the magnitude exponent increases gradually from 1.5 to 2. (d) The magnitude scaling exponent versus the analytical MF spectrum width,  $h_{\max} - h_{\min}$ . We summarize the log-normal distribution ( $\circ$ , Fig. 6c) and log-Poisson ( $\triangle$ , c). Both examples exhibit the same behavior of increasing magnitude exponent as a function of the MF spectrum width. We approximate this increase by  $1 + 1/(1 + e^{-17x})$  where  $x \equiv h_{\max} - h_{\min}$ .

numerical techniques [41]. In addition, it requires a long time series. Our analysis of the magnitude series is less sophisticated and is applicable to shorter time series. We note that a direct numerical calculation of the MF spectrum width from a time series may not follow the relation described in Fig. 7d due to (i) an overestimation of the MF spectrum width caused by the numerical technique for calculating the MF spectrum [and estimation of  $\tau(q \rightarrow \pm\infty)$ ] and (ii) a finite series length. However, we expect the magnitude scaling exponent to increase monotonically with the width of the MF spectrum [42].

## 6. Diagnostic utility of magnitude and sign scaling exponents on heartbeat interval series

In a previous study, we showed that statistics obtained from the magnitude and sign series of heartbeat increments can be used to separate healthy subjects from those with heart failure [26]. In that work, heartbeat interval records of up to 6 h,  $\approx 30,000$  points, were analyzed. Here, we show that an even shorter time series—of the order of 2000 points ( $\sim 1/2$  h)—can yield a significant separation between healthy individuals and those with heart failure.

Our analysis is based on 24 h Holter recordings from 18 healthy individuals (Fig. 4) and from 12 individuals with congestive heart failure (see footnote 8). We subdivide each record to segments of 1024 data points and use the DFA method to calculate the fluctuation function  $F(n)$ . We choose the scale  $n = 16$  to be the crossover point since it separates between a short-range regime ( $6 < n < 16$ ) with exponent  $\alpha_1$ , and an intermediate-range regime ( $16 \leq n \leq 64$ ) with exponent  $\alpha_2$ . We perform our scaling analysis for the original series, as well as the magnitude and sign sub-series. For each time segment we show the 1/2 h average scaling exponent of the healthy and heart failure groups (Fig. 8).

The short-range exponent  $\alpha_1$  of the original *RR* series (Fig. 8a) shows good separation between the healthy and heart failure groups [43]. During nighttime the healthy exponent drops towards the heart failure exponent. This might be related to the lower scaling exponent of interbeat interval series of healthy subjects during light and deep sleep episodes [15]. In addition, the heart failure group shows an apparent slow oscillatory-like behavior of two cycles per 24 h period. The intermediate exponent does not show a clear separation between the two groups.

The short and intermediate-range magnitude series exponents also distinguish between the interbeat patterns of healthy and unhealthy hearts (Fig. 8b). For short range, the scaling exponent for the heart failure group is systematically larger than for the healthy group while for the intermediate-range exponent we observe the opposite. Thus, there is a crossover behavior in the magnitude exponent both for healthy individuals and those with heart failure; this crossover might be related to the crossover of the interbeat intervals series [11] since the original, magnitude, and sign exponents depend on one another at small scales (Section 4). At larger scales ( $n > 64$ , not shown) the separation between healthy and unhealthy hearts is significant and might be related to the decrease of nonlinearity with disease [26].

The behavior of the sign series is similar to that of the original heartbeat increment series (Fig. 8c). The short-range exponent  $\alpha_1$  is larger for healthy subjects. In addition, the intermediate-range exponent separates between healthy individuals and those with heart failure; the exponent is smaller for the healthy. At night, the healthy tend to converge toward the heart failure—these changes might be related to the changes in the sign series during the different sleep stages [44]. We also observe here an apparent oscillatory-like behavior of two cycles per 24-h period.

In summary, we show that, in addition to the original *RR* series, the magnitude and sign sub-series may help to distinguish between the healthy group and the heart failure group. We also show that a short time series of order of 2000 points ( $\sim 1/2$  h) may

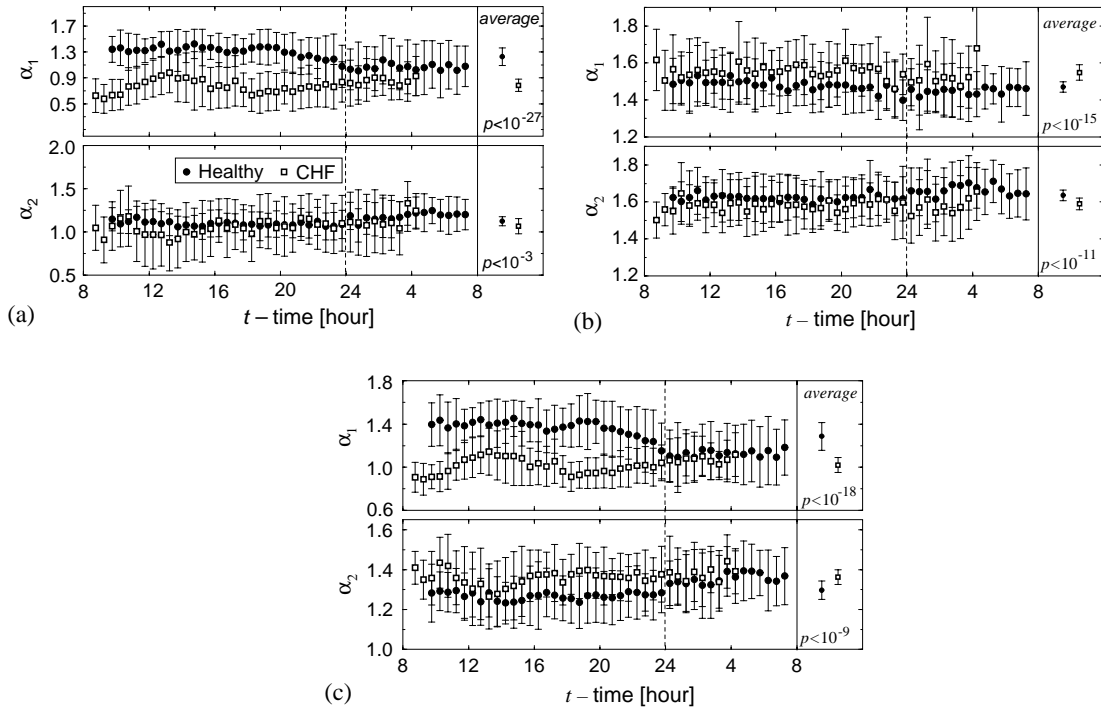


Fig. 8. Diagnostic implementation of the magnitude and sign decomposition. Here we show the different scaling exponents (original, magnitude, and sign), calculated from the interbeat interval series, as a function of daytime. We average the healthy group and the heart failure group; the average  $\pm 1$  standard deviation is shown. We calculate the scaling exponent in two regimes, short-range exponent,  $\alpha_1$  ( $6 \leq n < 16$ ), and intermediate-range scaling exponent,  $\alpha_2$  ( $16 \leq n < 64$ ). The vertical dashed line indicates midnight. The  $p$ -value for the group averages is obtained by the Student's  $t$ -test and is given in the right-hand side (for all measures  $p < 10^{-3}$ ). (a) The summary of the correlation properties of the original  $RR$  series. The short-range scaling exponent  $\alpha_1$  for the healthy group is significantly different from that of the heart failure group. Note that during sleep time there is larger overlap between the healthy and heart failure group. (b) The summary of the correlation properties of the integrated magnitude ( $|\Delta RR|$ ) series. The short-range scaling exponent for the healthy group is *smaller* than the heart failure group exponent. In the intermediate range, on the other hand, the exponent of the healthy group is larger than the exponent of the heart failure group indicating the presence of a crossover for the magnitude series. When considering several hours of recording during daytime the scaling exponent of the healthy group is significantly higher than that of the heart failure group indicating stronger long-term nonlinearity for the healthy individuals. (c) The summary of the correlation properties of the integrated sign ( $\text{sgn}(\Delta RR)$ ) series. The scaling exponent also exhibit significant separation. For short range the exponent for healthy is higher than the exponent for heart failure while for the intermediate range it is smaller than the exponent for heart failure. This is an indication for a crossover in the scaling of the sign series. During night the scaling exponent for healthy converges to the heart failure exponent.

yield a significant separation. The combination of several measures derived from the original, magnitude, and sign series might improve the diagnosis using short interbeat interval time series. Note that, in general, the fluctuation function at the crossover position  $F(n \approx 16)$  yields even more significant separation between healthy individuals and those with heart failure (not shown; see [16,26,43]).

## 7. Summary

We conclude that series with identical correlation properties can have completely different time ordering which can be characterized by different scaling exponents for the magnitude and sign series. The magnitude series reflects the way the series increments are clustered (volatility [25]) while the sign reflects the way they alternate. Moreover, we show that the magnitude series carries information regarding nonlinear properties of the original series while the sign series carries information regarding linear properties of the original series. The nonlinearity, as reflected by the magnitude series scaling exponent, is related to the width of the multifractal spectrum of the original series.

Application of the magnitude and sign decomposition on heartbeat increment series helps us to suggest a dynamical rule of healthy heartbeat increments—a big heartbeat increment in the positive direction is likely to be followed by a big increment in the negative direction. Moreover, the magnitude and sign scaling exponents may be used for diagnostic purposes. Because information obtained by decomposing the original heartbeat time series into magnitude and sign time series likely reflects aspects of neuroautonomic regulation, this type of analysis may help address the challenge of developing realistic models of heart rate control in health and disease.

## Acknowledgements

Partial support was provided by the NIH/National Center for Research Resources (P41 RR13622), the Israel-USA Binational Science Foundation, and the German Academic Exchange Service (DAAD). We thank L.A.N. Amaral, D. Baker, S.V. Buldyrev, A. Bunde, J.M. Hausdorff, R. Karasik, J.W. Kantelhardt, G. Paul, Y. Yamamoto, and especially to A.L. Goldberger for helpful discussions.

## Appendix A. Nonlinearity and multifractality

In this appendix we define the linearity and nonlinearity of a time series. We also review the relation between the multifractality of a time series and its nonlinearity.

Following Refs. [27,32] we define a time series to be *linear* if it is possible to reproduce its statistical properties from the power spectrum and the probability distribution alone, regardless of the Fourier phases [27]. This definition includes (i) autoregression processes

$$x_n = \sum_{i=1}^M a_i x_{n-i} + \sum_{i=0}^L b_i \eta_{n-i}, \quad (\text{A.1})$$

where  $\eta$  is Gaussian white noise and (ii) fractional Brownian motion [45]; the output,  $x_n$ , of these processes may undergo monotonic nonlinear transformations

$$s_n = s(x_n) \quad (\text{A.2})$$

and still be linear [27]. Processes which are not linear are defined as *nonlinear*. It is possible to destroy the nonlinearity of a time series by basically randomizing its Fourier phases (see Refs. [27,32] and Section 3).

A nonlinearity (linearity) of a time series is related to its multifractality. The definition of multifractality is based on the partition function  $Z_q(l)$  of a time series  $s_n$  and may be defined as [46]

$$Z_q(l) = \langle |s_{n+l} - s_n|^q \rangle, \quad (\text{A.3})$$

where  $\langle \cdot \rangle$  stands for expectation value. In some cases  $Z_q(l)$  obeys scaling laws

$$Z_q(l) \sim l^{\zeta_q}. \quad (\text{A.4})$$

If the exponents  $\zeta_q$  are linearly dependent on  $q$ , the series  $s_n$  is *monofractal*; if they are not,  $s_n$  is *multifractal*. (Note that in the present study we use a more advanced method to calculate multifractality that can accurately estimate the exponents of negative moments  $q < 0$  [41].)

The two-point correlation function of an increment time series  $\Delta s_n$  is defined as

$$A(l) = \langle \Delta s_n \Delta s_{n+l} \rangle. \quad (\text{A.5})$$

For long-range correlated stationary Gaussian time series

$$A(l) \sim l^{-\gamma}, \quad (\text{A.6})$$

where  $0 < \gamma < 1$ . In this case, the exponent  $\gamma$  is related to the DFA exponent  $\alpha$  of a  $\Delta s_n$  series by [47,48]

$$Z_2(l) \sim \langle s_n s_{n+l} \rangle \sim l^{2-\gamma} = l^{2\alpha}. \quad (\text{A.7})$$

In addition, these exponents are related to the power spectrum exponent,  $\beta$ , of the increment series  $\Delta s_n$

$$S(f) \sim 1/f^\beta \quad (\text{A.8})$$

by

$$\beta = 1 - \gamma = 2\alpha - 1. \quad (\text{A.9})$$

Thus, the second moment only depends on the power spectrum and is independent of the Fourier phases

$$\zeta_2 = 2\alpha = \beta + 1. \quad (\text{A.10})$$

For monofractal series [41,49],

$$\zeta_q = \alpha q = \frac{\beta + 1}{2} q. \quad (\text{A.11})$$

Thus, the MF spectrum of monofractal series is independent of the Fourier phases. This implies that (i) a long-range correlated series that has uncorrelated Fourier phases is monofractal and (ii) after randomizing the Fourier phases of an MF series it becomes monofractal [14].

In summary, monofractal series are linear since their statistical properties depend only on the power spectrum (two-point correlations) and the probability distribution.

On the other hand, MF series are nonlinear since their higher moments are not solely dependent on the probability distribution and the power spectrum, but also related to the Fourier phases.

## References

- [1] M.F. Shlesinger, *Ann. NY Acad. Sci.* 504 (1987) 214.
- [2] T. Vicsek, *Fractal Growth Phenomenon*, 2nd Edition, World Scientific, Singapore, 1993.
- [3] H. Takayasu, *Fractals in the Physical Sciences*, Manchester University Press, Manchester, UK, 1997.
- [4] C.-K. Peng, S.V. Buldyrev, A.L. Goldberger, S. Havlin, F. Sciortino, M. Simons, H.E. Stanley, *Nature* 356 (1992) 168.
- [5] C.-K. Peng, S.V. Buldyrev, S. Havlin, M. Simons, H.E. Stanley, A.L. Goldberger, *Phys. Rev. E* 49 (1994) 1685.
- [6] S.V. Buldyrev, A.L. Goldberger, S. Havlin, R.N. Mantegna, M.E. Matsu, C.-K. Peng, M. Simons, H.E. Stanley, *Phys. Rev. E* 51 (1995) 5084.
- [7] A. Arneodo, E. Bacry, P.V. Graves, J.F. Muzy, *Phys. Rev. Lett.* 74 (1995) 3293.
- [8] B. Audit, C. Thermes, C. Vaillant, Y. d'Aubenton-Carafa, J.F. Muzy, A. Arneodo, *Phys. Rev. Lett.* 86 (2001) 2471.
- [9] M. Kobayashi, T. Musha, *IEEE Trans. Biomed. Eng.* 29 (1982) 456.
- [10] C.-K. Peng, J. Mietus, J.M. Hausdorff, S. Havlin, H.E. Stanley, A.L. Goldberger, *Phys. Rev. Lett.* 70 (1993) 1343.
- [11] C.-K. Peng, S. Havlin, H.E. Stanley, A.L. Goldberger, *Chaos* 5 (1995) 82;  
C.-K. Peng, S. Havlin, J.M. Hausdorff, J.E. Mietus, H.E. Stanley, A.L. Goldberger, *J. Electrocardiol.* 28 (1995) 59.
- [12] K.K.L. Ho, G.B. Moody, C.-K. Peng, J.E. Mietus, M.G. Larson, D. Levy, A.L. Goldberger, *Circulation* 96 (1997) 842.
- [13] P.-A. Absil, R. Sepulchre, A. Bilge, P. Gerard, *Physica A* 272 (1999) 235.
- [14] P.Ch. Ivanov, L.A.N. Amaral, A.L. Goldberger, S. Havlin, M.G. Rosenblum, Z.R. Struzik, H.E. Stanley, *Nature* 399 (1999) 461.
- [15] A. Bunde, S. Havlin, J.W. Kantelhardt, T. Penzel, J.H. Peter, K. Voigt, *Phys. Rev. Lett.* 85 (2000) 3736.
- [16] Y. Ashkenazy, M. Lewkowicz, J. Levitan, S. Havlin, K. Saermark, H. Moelgaard, P.E. Bloch Thomsen, M. Moller, U. Hintze, H.V. Huikuri, *Europhys. Lett.* 53 (2001) 709.
- [17] S. Blesic, S. Milosevic, D. Stratimirovic, M. Ljubisavljevic, *Physica A* 268 (1999) 275.
- [18] J.M. Hausdorff, C.-K. Peng, Z. Ladin, J.Y. Wei, A.L. Goldberger, *J. Appl. Physiol.* 78 (1995) 349;  
J.M. Hausdorff, S.L. Mitchell, R. Firtion, C.-K. Peng, M.E. Cudkowicz, J.Y. Wei, A.L. Goldberger, *J. Appl. Physiol.* 82 (1997) 262.
- [19] J.D. Pelletier, *J. Climate* 10 (1997) 1331.
- [20] E. Koscielny-Bunde, A. Bunde, S. Havlin, H.E. Roman, Y. Goldreich, H.-J. Schellnhuber, *Phys. Rev. Lett.* 81 (1998) 729.
- [21] P. Talkner, R.O. Weber, *Phys. Rev. E* 62 (2000) 150.
- [22] K. Ivanova, M. Ausloos, *Physica A* 274 (1999) 349.
- [23] K. Ivanova, M. Ausloos, E.E. Clothiaux, T.P. Ackerman, *Europhys. Lett.* 52 (2000) 40.
- [24] R.N. Mantegna, H.E. Stanley, *Nature* 376 (1995) 46.
- [25] Y. Liu, P. Gopikrishnan, P. Cizeau, M. Meyer, C.-K. Peng, H.E. Stanley, *Phys. Rev. E* 60 (1999) 1390.
- [26] Y. Ashkenazy, P.Ch. Ivanov, S. Havlin, C.-K. Peng, A.L. Goldberger, H.E. Stanley, *Phys. Rev. Lett.* 86 (2001) 1900.
- [27] T. Schreiber, A. Schmitz, *Physica D* 142 (2000) 346.
- [28] J.W. Kantelhardt, E. Koscielny-Bunde, H.H.A. Rego, S. Havlin, A. Bunde, *Physica A* 295 (2001) 441.
- [29] K. Hu, P.Ch. Ivanov, Z. Chen, P. Carpena, H.E. Stanley, *Phys. Rev. E* 64 (2001) 011114;  
Z. Chen, P.Ch. Ivanov, K. Hu, H.E. Stanley, *Phys. Rev. E* 65 (2002) 041107.
- [30] Y. Ashkenazy, P.Ch. Ivanov, S. Havlin, C.-K. Peng, Y. Yamamoto, A.L. Goldberger, H.E. Stanley, *Comput. Cardiology* 27 (2000) 139.

- [31] A. Babloyantz, P. Maurer, *Phys. Lett. A* 221 (1996) 43;  
P. Maurer, H.-D. Wang, A. Babloyantz, *Phys. Rev. E* 56 (1997) 1188.
- [32] T. Schreiber, A. Schmitz, *Phys. Rev. Lett.* 77 (1996) 635.
- [33] P.F. Panter, *Modulation, Noise, and Spectral Analysis Applied to Information Transmission*, McGraw-Hill, New York, NY, 1965.
- [34] J. Theiler, S. Eubank, A. Longtin, B. Galdrikian, J.D. Farmer, *Physica D* 58 (1992) 77.
- [35] J. Kurths, A. Voss, P. Saparin, A. Witt, H.J. Kleiner, N. Wessel, *Chaos* 5 (1995) 88;  
A. Voss, N. Wessel, H.J. Kleiner, J. Kurths, R. Dietz, *Nonlinear Anal.-Theor.* 30 (1997) 935.
- [36] G. Sugihara, W. Allan, D. Sobel, K.D. Allan, *Proc. Natl. Acad. Sci. USA* 93 (1996) 2608.
- [37] A. Arneodo, E. Bacry, J.F. Muzy, *J. Math. Phys.* 39 (1998) 4142;  
A. Arneodo, S. Manneville, J.F. Muzy, *Euro. Phys. J. B* 1 (1998) 129.
- [38] I. Daubechies, *Ten Lectures on Wavelets*, SIAM, Philadelphia, PA, 1992.
- [39] W.H. Press, S.A. Teukolsky, W.T. Vetterling, B.P. Flannery, *Numerical Recipes in C*, 2nd Edition, Cambridge University Press, Cambridge, MA, 1995.
- [40] E. Bacry, J. Delour, J.F. Muzy, *Phys. Rev. E* 64 (2001) 026 103.
- [41] J.F. Muzy, E. Bacry, A. Arneodo, *Int. J. Bifurcat. Chaos* 4 (1994) 245.
- [42] Y. Ashkenazy, J.M. Hausdorff, P.Ch. Ivanov, H.E. Stanley, *Physica A* 316 (2002) 662.
- [43] Y. Ashkenazy, M. Lewkowicz, J. Levitan, S. Havlin, K. Saermark, H. Moelgaard, P.E.B. Thomsen, *Fractals* 7 (1999) 85.
- [44] J.W. Kantelhardt, Y. Ashkenazy, P.Ch. Ivanov, A. Bunde, S. Havlin, T. Penzel, J.-H. Peter, H.E. Stanley, *Phys. Rev. E* 65 (2002) 051 908.
- [45] B.B. Mandelbrot, J.W. Van Ness, *SIAM Rev.* 10 (1968) 422–437.
- [46] A.L. Barabasi, T. Vicsek, *Phys. Rev. A* 44 (1991) 2730.
- [47] M.S. Taqqu, V. Teverovsky, W. Willinger, *Fractals* 3 (1995) 785.
- [48] H.A. Makse, S. Havlin, M. Schwartz, H.E. Stanley, *Phys. Rev. E* 53 (1996) 5445.
- [49] J.F. Muzy, E. Bacry, A. Arneodo, *Phys. Rev. E* 47 (1993) 875.